Catal Lett (2012) 142:1295–1305
DOI 10.1007/s10562-012-0910-5

Hydrocracking and Hydroisomerization of *n*-Hexadecane, *n*-Octacosane and Fischer–Tropsch Wax Over a Pt/SiO_2–Al_2O_3 Catalyst

Jungshik Kang · Wenping Ma · Robert A. Keogh · Wilson D. Shafer · Gary Jacobs · Burtron H. Davis

Received: 13 August 2012 / Accepted: 12 September 2012 / Published online: 3 October 2012

Abstract The hydroisomerization and hydrocracking of long chain *n*-paraffins and a Fischer–Tropsch wax produced with a cobalt catalyst were accomplished over a Pt–amorphous silica–alumina catalyst. The relative conversion of the *n*-hexadecane and *n*-octacosane mixed feed greatly favored the higher carbon number compound even though the conversions of the pure hydrocarbons were the same within a factor of two or less when converted separately. Thus, vapor equilibrium plays a role for the conversion of the heavier alkanes and in this case the conversion essentially occurs with only the compound present in the liquid phase. The single branched cracked products show a peak at the mid-carbon number, C_8 and C_{14} for the two reactants, but the peak for the multi-branched product occurs at a higher carbon number. Thus, it appears that the multi-branched products are primarily produced in a series reaction with the singly branched compounds being formed as the primary products. The data for wax conversion are consistent with the competitive conversion operating for the higher carbon number compounds; however, the transport of intermediate carbon number products from the reactor occurs more rapidly than their formation rates by cracking reactions. The data clearly show that the hydrocracking of wax is dominated by vapor–liquid equilibrium and that hydrocracking is initially controlled by the compounds present in the liquid phase.

J. Kang · W. Ma · R. A. Keogh · W. D. Shafer · G. Jacobs · B. H. Davis (✉)
Center for Applied Energy Research, University of Kentucky, 2540 Research Park Dr., Lexington, KY 40511, USA
e-mail: burtron.davis@uky.edu

Keywords Hydrocracking · Hydroisomerization · Pt/silica–alumina · *n*-Hexadecane · *n*-Octacosane · Fischer–Tropsch wax · Iso/normal ratio

1 Introduction

The hydrocracking and hydroisomerization of long chain paraffins over bifunctional catalysts are receiving increasing attention. A driving force for current research is the search to develop economical ways to utilize both the heavier residuals of petroleum and tar sand bitumen, as well as FT wax; moreover, there are increasing efforts to provide more environmentally friendly ways to perform refining [1]. Recent commercial FT plants utilize low temperature synthesis and this operation produces products that favor higher carbon number waxes. One approach to convert the waxes to transportation fuels is hydrocracking [2, 3]. Hydrocracking was developed in Germany in the 1930s as part of their direct coal liquefaction program. However, it remained until the late 1950s when more active catalysts were developed (especially by Chevron and Union Oil) for this process to be firmly established.

Many of the steps in the reaction mechanisms of hydrocracking are understood in a general way, even though details are still unknown. The general consensus is that hydrocracking is based on the catalytic formation of carbenium ions to break carbon–carbon bonds and generate olefinic bonds [3]. The hydrocracking reaction pathway can thus be described by Scheme 1 in which hydrocracking and isomerization occur competitively [4–10]. Generally, a bifunctional catalyst [11–15] consisting of transition or noble metals supported on acidic oxides are applied to a conventional hydrocracking process, and these are capable of rearranging and breaking carbon–carbon bonds, as well

Scheme 1 Hydrocracking reaction pathway on a conventional bifunctional catalyst

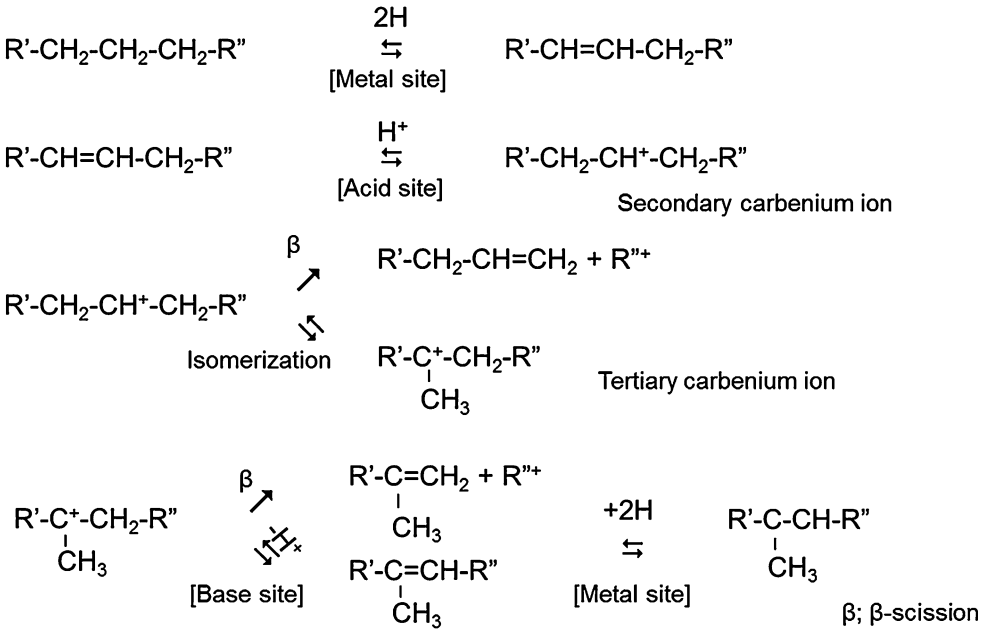

as adding hydrogen to aromatics and olefins to produce naphthenes and alkanes.

In Scheme 1 the metal site provides the dehydrogenation function to convert the alkane to an alkene (and vice versa), while the acid function effects the isomerization and/or cracking through a carbocation intermediate [16–18].

In this study, the hydrocracking characteristics of *n*-hexadecane (*n*-C_{16}), *n*-octacosane (*n*-C_{28}), their equimolar mixture and cobalt-derived FT wax were studied using a 0.5 wt% Pt/amorphous silica–alumina catalyst. The hydrocracking characteristics of a cobalt catalyst-derived Fischer–Tropsch wax were defined for various operating conditions. The wax conversion, product selectivity, and degree of isomerization of the wax components for various reaction conditions were determined.

2 Experimental

The silica–alumina support (coarse grade 135) was purchased from Davison Chemical. The 0.5 wt% Pt/SiO_2–Al_2O_3 catalyst was prepared by the incipient wetness impregnation method. Tetraammine platinum(II) nitrate (Alfa Aesar, Pt 50.38 %) was used as the platinum precursor. Following impregnation and drying, the catalyst was calcined in air at 500 °C for 4 h at atmospheric pressure.

The surface area, pore volume, and pore size of commercial support and Pt/Si–Al catalyst were measured by BET using a Micromeritics Tri-Star system. Prior to the measurements, samples were slowly ramped to 160 °C and evacuated for 24 h to approximately 50 mTorr.

Hydrogen chemisorption measurements were performed using a Zeton Altamira AMI-200 unit to determine the metal dispersion of the catalyst. The catalyst was activated at 400 °C for 1 h using 30 cm^3/min of 33 %H_2/He and then cooled under flowing hydrogen to 80 °C. The sample was then held at 80 °C under flowing argon to prevent physisorption of weakly bound species prior to increasing the temperature slowly to the activation temperature. The TPD spectrum was integrated and the number of moles of desorbed hydrogen determined by comparing to the areas of calibrated hydrogen pulses.

Hydrocracking of *n*-hexadecane, *n*-octacosane and FT wax were performed in a fixed-bed reactor made from 314 stainless steel. The reactor has a 1 in. inner diameter and is 22 in. in length. An appropriate amount of catalyst (0.25–3 g) was diluted with 2 and 8 g of 1 and 3 mm diameter glass beads. The catalyst was activated at 400 °C, 15 Nl/h H_2 and 1 atm for 14 h prior to the hydrocracking reaction. After activation, the reactor temperature was slowly decreased to the reaction temperature, and the reactor was pressurized to the desired pressure with H_2 prior to feeding the reactant.

Ultra high purity H_2 gas flow was controlled by a precalibrated Brooks mass flow controller. An ISCO syringe pump was used to feed *n*-hexadecane (Alfa Aesar, <99 %) and/or *n*-octacosane (Alfa Aesar, 99 %). The cobalt-derived FT wax was melted in a 600 ml heating vessel and suctioned into a high temperature ISCO syringe pump before it was fed to the reactor at the desired flow rate through a heated line (150 °C). During the hydrocracking reaction, the molar ratio of H_2/hydrocarbon (feed) was maintained at 20, the reaction pressure was varied from 150 to 600 psig (10.2–40.8 atm), the liquid hourly space velocity (LHSV) was in the range of

Table 1 Physical properties of support and Pt catalyst used in this work

Catalyst description	BET SA (m^2/g)	Single point pore volume (cm^3/g)	Average single point pore radius (nm)
SiO_2–Al_2O_3	395	0.664	3.5
0.5 wt% Pt/SiO_2–Al_2O_3	358	0.600	3.4

1–10 and the reaction temperature was varied from 230 to 310 °C. The H_2/reactant for the wax was based on the average molecular weight of the wax.

The effluent gas passed through hot (160 °C) and cold (4 °C) traps to condense the liquid products. The exit gas flow was measured using a bubble flow meter and the gaseous products were collected in a 1 l gas sampling bag for analysis. Gaseous products were analyzed using a micro GC with a thermal conductivity detector (TCD). HP 5890 and HP 6890 GCs with flame ionization detectors (FID) were used for analysis of the liquid and solid samples using DB-5 and HT-5 columns. Samples from the reactor were collected after steady-state conditions were reached. Generally, an interval of about 24 h was allowed following each change of reaction conditions before a sample was collected. The condensed light hydrocarbons were kept refrigerated prior to analysis. Gas samples were analyzed immediately after collection.

The wax conversion and selectivity for naphtha and diesel are arbitrarily defined as carbon number change based on carbon moles. The conversion and product selectivity are defined below:

For FT wax hydrocracking:

$$\text{Wax conversion} = ((C_{20+} \text{ in the feed} - C_{20+} \text{ in the product})/C_{20+} \text{ in feed}) \times 100$$

For long chain hydrocarbon (n-C_{16} and n-C_{28}) hydrocracking:

$$\text{Cracking conversion} = ((C_n\text{-Feed} - C_n \text{ in the product})/C_n\text{-Feed}) \times 100 \text{ and}$$

$$\text{Iso selectivity} = ((iC_n \text{ in the product})/(C_n\text{-Feed} - C_n \text{ in the product})) \times 100.$$

3 Results

Characterization results of BET surface area and porosity are listed in Table 1. The pore size distribution shows an envelope shape in 1 to 10 nm range and the highest peak is around 3.5 nm, as shown in Fig. 1. After loading Pt onto commercial Si–Al support, the surface area slightly decreased; however, the pore volume and pore size did not change significantly. Regarding hydrogen chemisorption, the average diameter of the catalyst was 1.5 nm, which corresponds to a metal dispersion of 78.2 %.

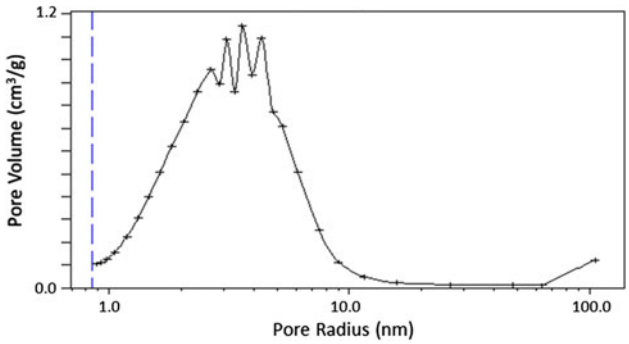

Fig. 1 Pore size distribution on 0.5 wt% Pt/SiO_2–Al_2O_3

The conversion and isoalkane selectivity data for *n*-hexadecane and *n*-octacosane conversion at various temperatures are shown in Fig. 2. For both reactants the selectivity for isomerization to methyl substituted alkanes is high (>90 %) but declines with increasing temperature. The fraction of conversion represented by cracking at any temperature is higher for *n*-octacosane than for *n*-hexadecane. At a given temperature, the conversion varied with space velocity with *n*-octacosane showing a slightly higher conversion (Fig. 3). The relative conversion of C_{28}/C_{16} with increasing LHSVs are: LHSV 2, 2.36; LHSV 4, 2.0; LHSV 6, 1.75; LHSV 8, 1.44 and LHSV 10, 1.24. Thus, with increasing space velocity the relative conversion approaches unity, suggesting an approach to a nearly equal conversion rate for each compound. This suggests that the liquid film of *n*-octacosane is responsible for at least some of the higher conversion of *n*-octacosane at the lower space velocities. This implies that the predominantly gas phase conversion of pure *n*-hexadecane and the liquid phase of pure *n*-octacosane are nearly, or are, equal at the higher space velocity. However, this is not the case when the two reactants are converted when an equimolar mixture of these two reactants are used. As shown in Fig. 4, the amount of *n*-hexadecane in the products is high enough that the C_{16} conversion is negative. However, if it is assumed that the C_{16} products from *n*-octacosane cracking are the same as for the C_{15} and C_{17} products, then the conversion of *n*-hexadecane is slightly positive (Fig. 4).

These competitive conversion results indicate that the catalyst pore is essentially filled with the higher boiling reactant (Fig. 5). Thus, for the cracking of wax only the higher molecular weight products should be converted until

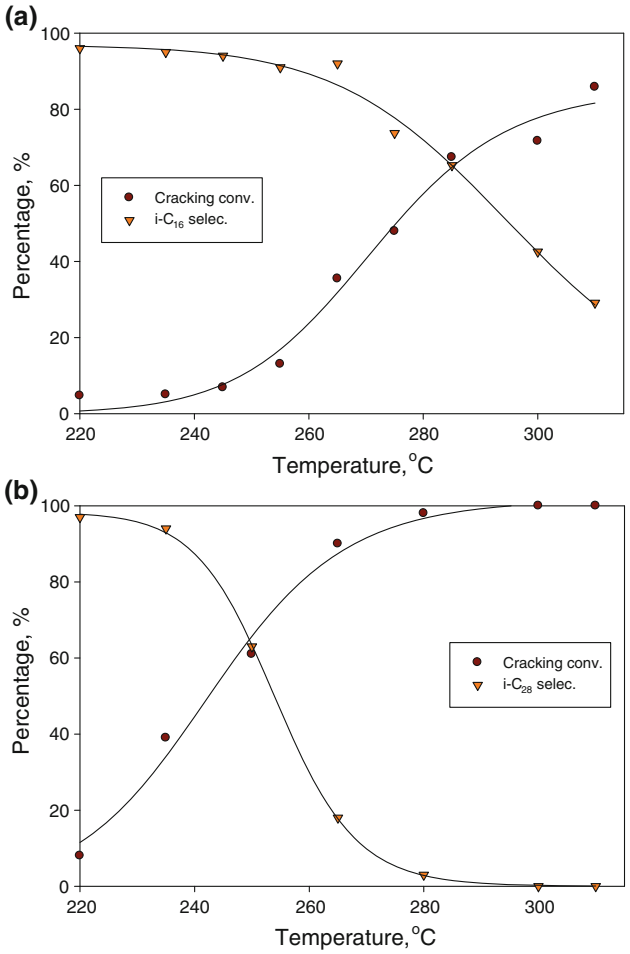

Fig. 2 Conversion and selectivity of long chain hydrocarbons (**a** n-C_{16} and **b** n-C_{28}) hydrocracking at various reaction temperatures (at 450 psig, LHSV = 2 h^{-1})

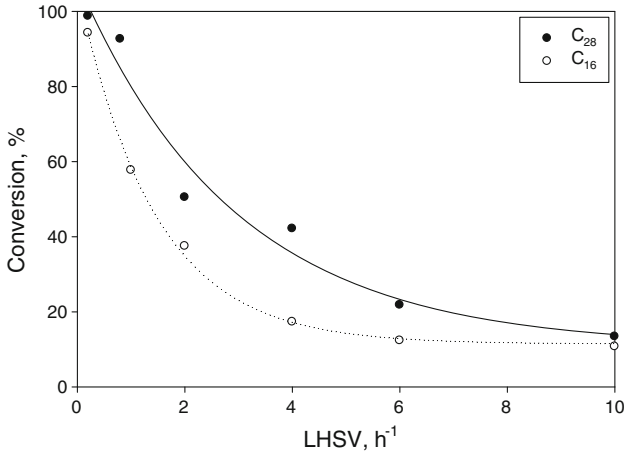

Fig. 3 Conversion versus LHSV of n-C_{16} and n-C_{28} each feeds at 280 °C, 450 psig

a very high conversion is attained for the higher carbon number components of the wax. This means that the products that are produced from cracking of the heavy wax

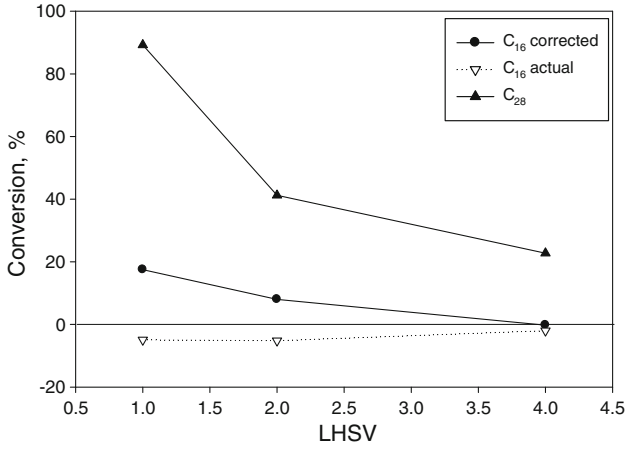

Fig. 4 Conversion versus LHSV of the n-C_{16} and n-C_{28} mixture feed at 280 °C, 450 psig

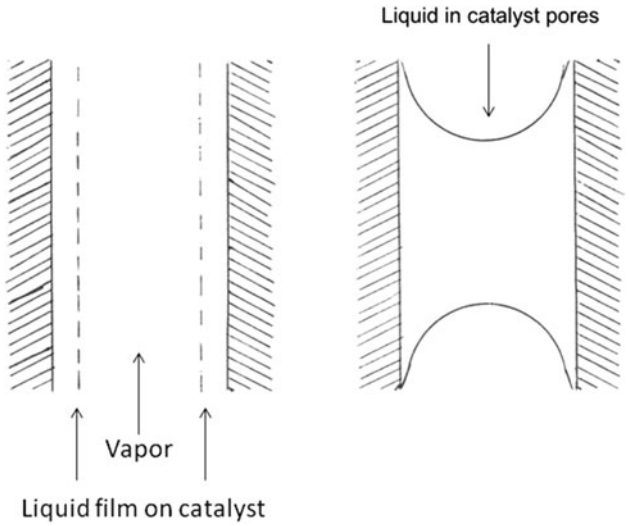

Fig. 5 Schematic of catalyst pore filling with low boiling alkane (*left*) and high boiling alkane (*right*)

products will not undergo secondary reactions once they exit the particle where they were formed and enter the vapor phase. In addition, the light products ($<C_{20–25}$) should pass through the hydrocracking reactor without undergoing secondary conversion. Over zeolite SSZ-16, n-hexane was reported to inhibit the hydrocracking of n-hexadecane due to shape selectivity [19, 20]. Lu et al. [21] also reported that the cracking of n-hexadecane in a 50/50 (v/v) mixture of n-C_8 and n-C_{16} was greatly suppressed using zeolite catalysts, which the authors referred to as "secondary shape selectivity." The reason for this term is that the cracking selectivity of the zeolite is affected by one of the reactants, and in this case the lower-carbon-number alkane inhibits the conversion of the higher-carbon-number alkane. Thus, we are not observing this type of secondary shape selectivity, but one that appears to depend on reactant vapor pressure.

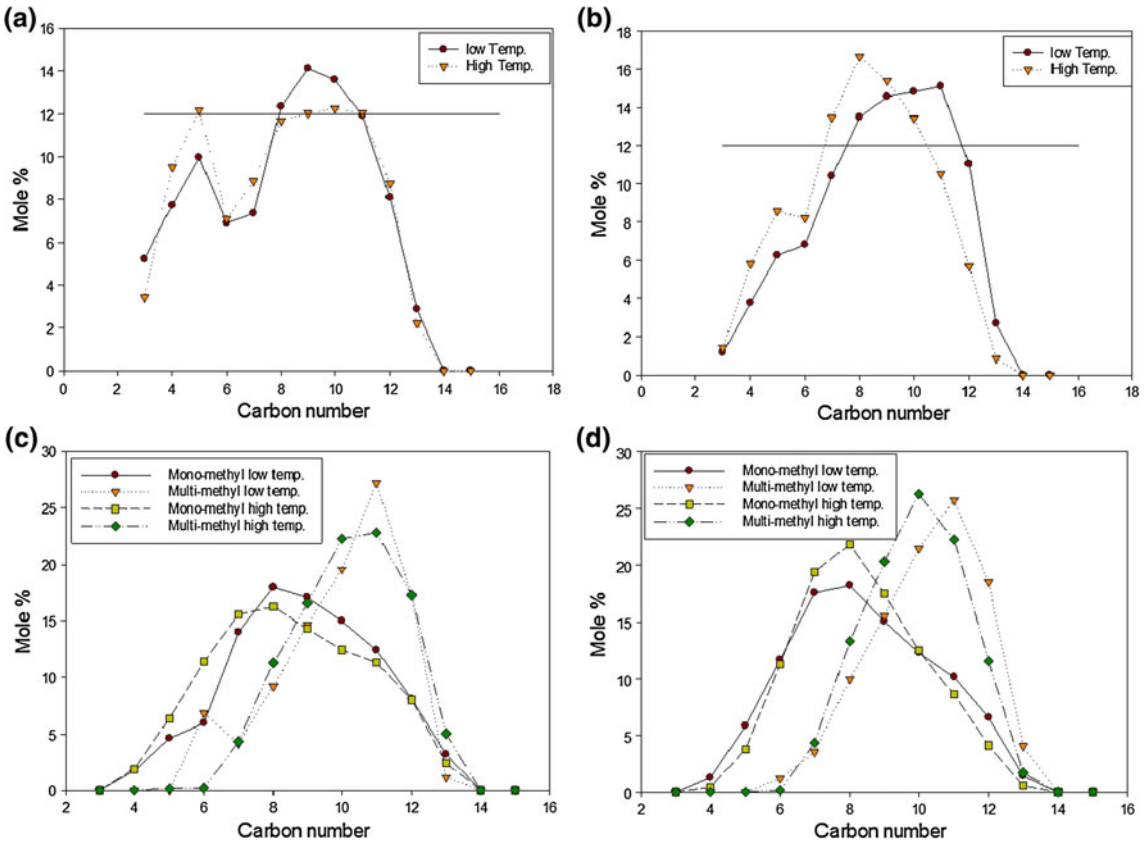

Fig. 6 *n*-Hexadecane cracking products for low (**a** 11 %) and high (**b** 70 %) conversion and the mono- and multi-branched cracking products at low (**c** low conversion; low and high temperatures) and high (**d** high conversion; low and high temperatures) conversions

The distribution of the cracked products is illustrated in Fig. 6 where the mono-branched and multi-branched products are shown. At both low and high conversion at low and high temperature conditions, the product distribution exhibits a peak at about carbon number 8 and a second peak at carbon number 5, presumably due to secondary cracking (Fig. 6a, b). The distributions for the mono- and the multi-branched products, each based on 100 % for the total components of each grouping (Fig. 6c, d), do not peak at the same carbon number. Surprisingly, the product distribution is such that the multi-branched cracked products have a higher average carbon number distribution than the mono-branched products; this is the case at both low and high (11 and 70 %) *n*-hexadecane conversion. The product distribution for mono-methylalkanes is bell-shaped and peaks at C_8, the carbon number peak expected for center-cracking. The peak for the multi-branched products is at C_{11} and is skewed toward the lower carbon-number products; thus, the formation and cracking of the multi-branched product appears to be impacted by the first substituent. As shown in Table 2, for *n*-hexadecane the multi-methyl isomers make up 20–30 mol% of the total cracked products. Thus, the isomerization to produce multi-methyl products is at least 1/4th the combined rates for the cracking and isomerization to mono-methyl products, and is likely significantly higher than this. For *n*-octacosane the multi-branched isomers comprise 40–45 % of the isoproducts, almost twice the amount for the conversion of *n*-hexadecane. Since many studies show that cracking of the branched alkane is more rapid than that of the normal isomer, this is a surprising result.

Table 2 Branched hydrocarbons of *n*-C_{16} and *n*-C_{28} over Pt/Si–Al catalyst at different conversion ranges

Feed (conversion)	Mono-methyl (mol %)		Multi-methyl (mol %)	
	High temp.	Low temp.	High temp.	Low temp.
n-C_{16} (11 %)	78.3	70.1	21.7	29.9
n-C_{16} (70 %)	71.9	73.0	28.1	27.0
n-C_{28} (23 %)	56.6	59.0	43.4	41.0
n-C_{28} (100 %)	55.2	55.5	44.8	44.5

The low conversion data for *n*-octacosane (Fig. 7a) approaches a constant number of moles of products versus carbon number, indicating that most interior C–C bonds have a similar cracking probability. However, with

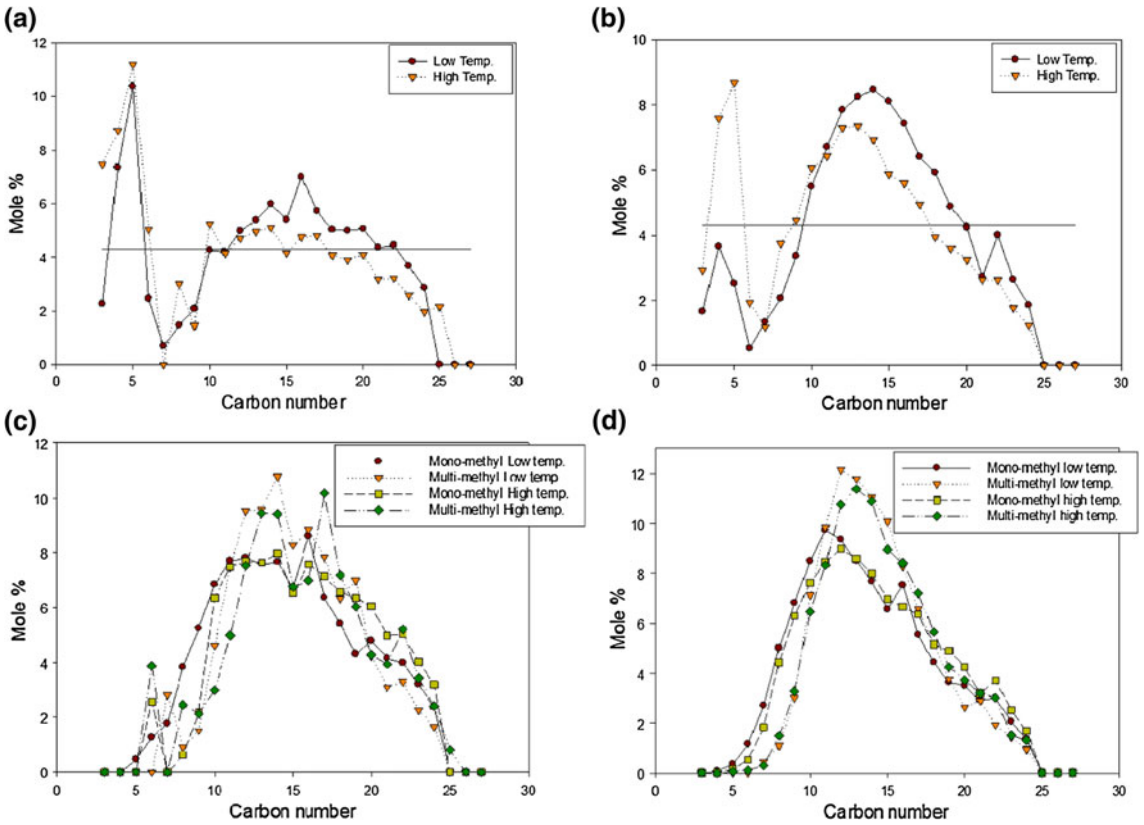

Fig. 7 *n*-Octacosane cracking products for low (**a** 23 %) and high (**b** 100 %) conversion and the mono- and multi-branched cracking products at low (**c** low conversion; low and high temperatures) and high (**d** high conversion; low and high temperatures) conversions

increasing conversion this shifts to a near-bell shaped curve with a peak at about C_{14}, as expected, although in this case it is skewed to the higher carbon number products. At both low and high temperature the mono-methyl and multi-methyl isomers exhibit a bell-shaped curve, with a slight skewing to higher molecular weight products as observed in the previous case of *n*-hexadecane hydrocracking. Because of overlap of g.c. peaks, the distributions within the methyl-substituted products have not been determined.

Figure 8 shows the reaction pathway and selectivity for isoalkane and cracked products formation for n-hexadecane and *n*-octacosane. For our data, it is apparent that the two reactants follow a single reaction pathway; that is, the selectivity for isomerization and cracking is the same over the total reactant conversion range. Thus, it appears that the same reaction pathway applies for the gas and liquid phase conversion of the reactants. This is also true for the data of Calemma et al. [17], except the authors obtained less cracking at higher conversion levels.

The fraction of branched products from the cracking reaction exceeds 0.8 for the higher carbon number products (Fig. 9). A similar fraction was obtained for *n*-hexadecane, *n*-octacosane and an equimolar mixture of these two reactants. Cracking of the carbocation of the *n*-alkane should produce only normal products. Thus, it appears that the cracking reaction occurs through the protonated dialkylcyclopropane or the methyl alkane carbocation; however, this would still produce only 0.5 fraction of branched products since one of the cracking fragments would have the n-alkane (or alkene) structure. The fact that the ratio of iso/normal products is 0.80 or higher means that the alkene formed by the normal cracking mechanism must undergo isomerization before it is hydrogenated (Scheme 2). This most likely occurs through the same mechanism that is followed for the bifunctional mechanism except it appears that the alkene that is formed undergoes isomerization to a branched isomer prior to being hydrogenated to the *n*-alkane. If the alkenes, especially the lower molecular weight ones that are formed from *n*-octacosane, were hydrogenated by competitive adsorption they should not be converted to isoalkanes. Only the lower (ca. C_{7}–) products show a fraction that falls below 0.80 and this is likely due, at least in part, to the lower reactivity of the C_{7}– isomers.

The reaction pathway outlined in Scheme 2 would be expected to produce more of the 2-methyl alkane than the other methyl substituted isomers. In the initial cracking step we would expect the methyl-branched isomer to be a 2-methyl isomer and this would require at least 0.5 of the

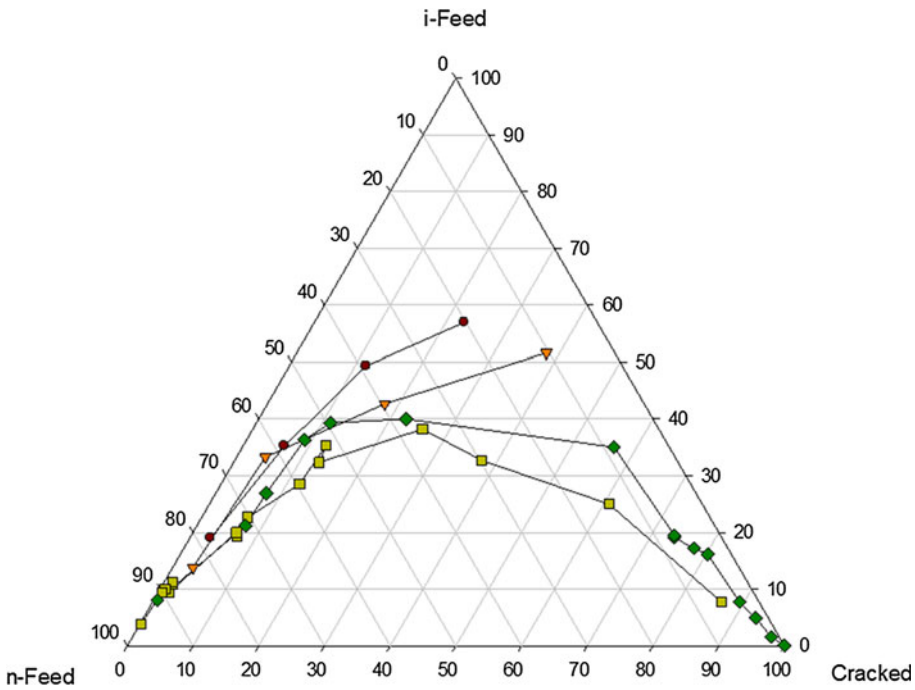

Fig. 8 Ternary plot of C_{16} (*light green square*) and C_{28} (*dark green diamond*) hydrocracking results. Reaction conditions were *n*-C_{16}; LHSV = 0.4 ~ 10, 280 °C, *n*-C_{28}; LHSV = 0.4 ~ 6, 270 °C and other reaction conditions were 450 psig. Also shown are results for C_{16} (*brown circle*) and C_{28} (*orange inverted triangle*) from Ref. [17]

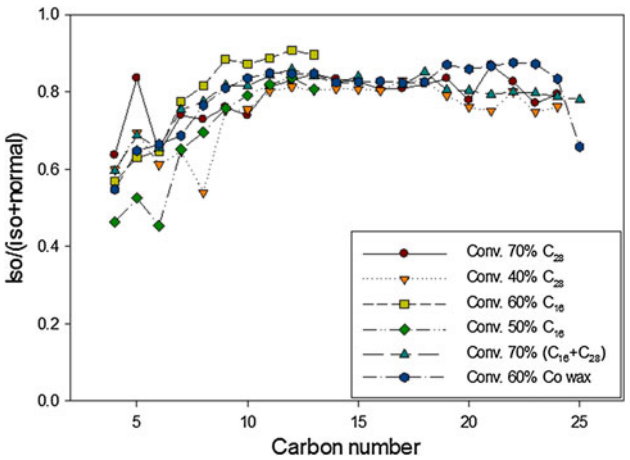

Fig. 9 Iso/(iso + normal) ratio over Pt/silica–alumina catalyst with various feeds within a conventional conversion range

branched isomers to be the 2-methyl isomer. As indicated in Fig. 10, while the 2-methyl isomer is a dominant one, it does not exceed that of the 3-methyl isomer. There is the expected decline in the methyl isomer fraction when the substitution is at the 4 position and higher. This indicates that there is some methyl migration in the methyl-alkene that is formed but that its occurrence falls far short of producing an equilibrium or statistical distribution. Furthermore, the position distribution of the methyl isomers is essentially the same for n-hexadecane, *n*-octacosane and for the mixture of these two compounds. If isomerization was the dominant factor in determining the distribution of the methyl isomers, we would expect the curve for the *n*-octacosane products to lie above the curve for the *n*-hexadecane products. Since it does not, it indicates that the methyl migration down the chain occurs at about the same rate for both reactants.

The i/*n* ratio of the products is very high (>60) for cracked products at 220 °C but decreases rapidly as the temperature increases (Fig. 11). Unfortunately, these data were not obtained at the same conversion level so that this may contribute to the trend shown in Fig. 11.

The conversion of FT wax produced using a Co-alumina catalyst was accomplished at various temperatures under the same reaction conditions (450 psig, LHSV = 1, H_2 flow = 1.4 Nl/h) as was used for *n*-hexadecane and *n*-octacosane. Increasing the temperature from 250 to 310 °C provided a conversion of 13 to 100 % when conversion is defined on the basis of the conversion of C_{20+} to lower carbon number products (Table 3). At the lower temperatures, and lower conversion, the products were predominantly in the diesel range (Fig. 12); however, for the reaction conditions used, the selectivity to diesel rapidly declined for reaction temperatures above about 280 °C. As shown in Fig. 9, the isoalkane fractions for the products are essentially the same as for the conversion of *n*-hexadecane and *n*-octacosane. Thus, for the conversion of waxes the isomerization of the alkene products appears to be as, or more, rapid than their hydrogenation to alkanes.

At low (150 psig) pressure the conversion is low but above about 300 psig the conversion attains a value where further increase in pressure does not impact the conversion (Table 4). Presumably the shorter residence time in the catalyst bed contributes to the lower conversion at 150 psig and the equilibrium concentration of alkenes together with

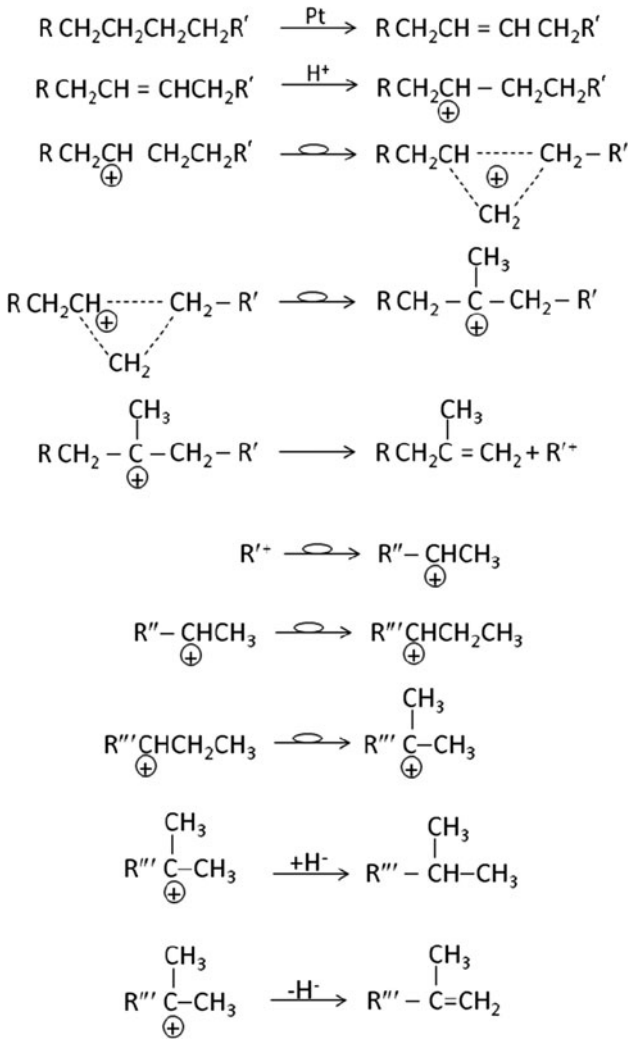

Scheme 2 Reaction pathway via protonated cyclopropane carbenium ion rearrangement to produce 2-methyl alkane

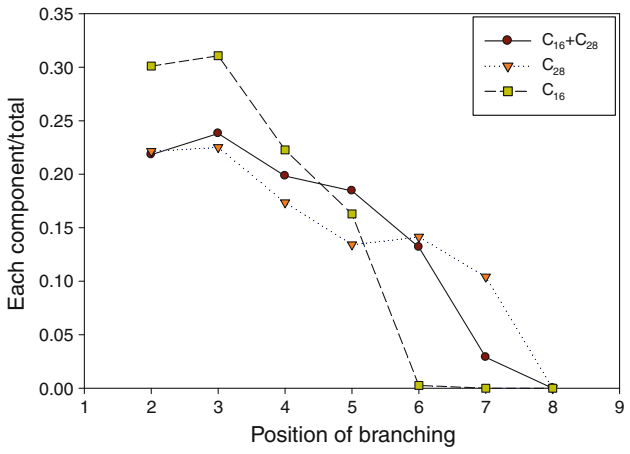

Fig. 10 Position of methyl group in the cracked products from the conversion of *n*-hexadecane, *n*-octacosane and an equimolar mixture of the two alkanes

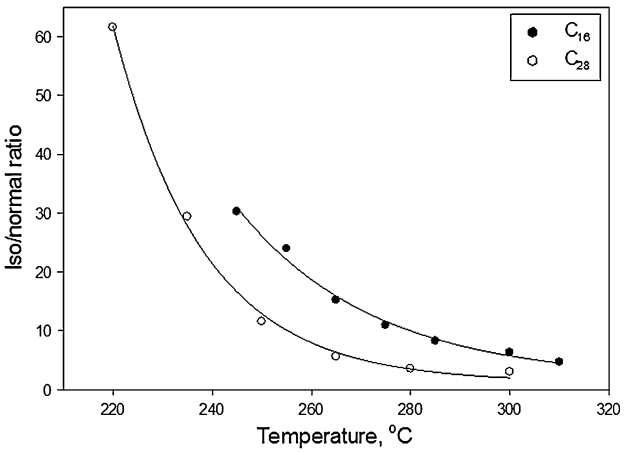

Fig. 11 Iso/normal ratio versus reaction temperature of C_{16} and C_{28} feeds over Pt/Si–Al catalyst

essentially saturation coverage of the acid sites is responsible for the lack of dependence of conversion on pressure above about 300 psig.

As expected, increasing the LHSV caused a decrease in conversion. At the low space velocity of 1 the conversion is essentially 100 % and the products fall primarily in the naphtha range (Fig. 13). As the space velocity is increased the diesel fraction increases so that at LHSV = 10 about 90 % of the cracked transportation fuel products fall in the diesel range as shown in Table 5. The data clearly show that the production of the desirable product, diesel, will be a matter of choice that depends upon the conversion rate and diesel selectivity that one finds acceptable for the process.

For the lighter alkanes, the catalyst pores may contain a liquid film covering each catalyst particle (Fig. 5 (left)). However, with increasing molecular weight a point will be reached where essentially all of the higher carbon number components of the wax will be present in the liquid phase; for this situation the catalyst pores will be filled with the liquid (Fig. 5 (right)). Even so, the void between the catalyst particles should not be filled with liquid and the lighter products, once they exit the catalyst particle, will leave the reactor quickly as was demonstrated by the conversion of the pure *n*-hexadecane and n-octacosane compounds and their mixture. For the wax, we would expect the heavier products (e.g., C_{30+}) to be present essentially in the liquid phase. We further expect that for these liquid components, adsorption on the catalyst acid sites will be essentially the same for each carbon number compound. If this expectation is true, then the conversion of the higher carbon number wax components should be directly related to their fraction in the mixture. Thus, in a plot of the change in concentration of each component, the higher molecular weight compounds should show the same conversion. For the conversion at different temperatures we

Table 3 The effect of temperature on FT wax hydrocracking reaction

Temp.(°C): Cracking HC (wt%)	250	270	280	290	300	310
C_2–C_3	0	0	0.01	0.03	0.21	0.20
C_4–C_{11} (naphtha)	0.36	0.69	2.22	33.5	97.8	98.9
C_{12}–C_{19} (diesel)	23.4	28.9	48.7	52.4	1.97	0.90
C_{20+}	76.2	70.4	49.1	14.1	0	0
Diesel/naphtha ratio	65.0	41.9	21.9	1.56	0.02	0.01
Wax conversion (%)	13	22	46	84	95	100

Pressure = 450 psig, LHSV = 1

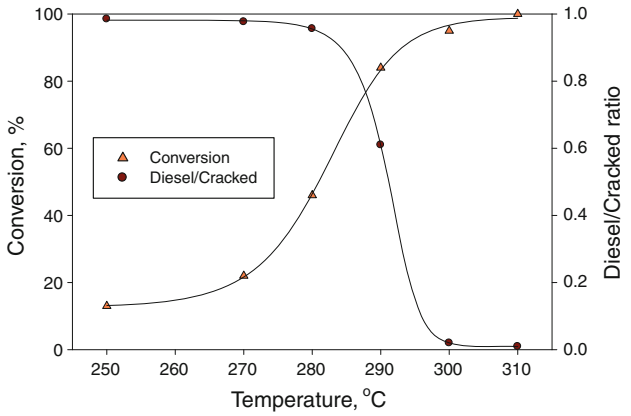

Fig. 12 Conversion of Co-catalyst derived wax (*orange triangle*) and the ratio of (diesel/(diesel + naphtha)) (*brown circle*)

Table 4 The effect of pressure on hydrocracking reaction of FT products over Pt/silica–alumina catalyst

Pressure (psig): Cracking HC (wt%)	600	450	300	150
C_2–C_3	0.16	0.15	0.14	0.07
C_4–C_{11} (naphtha)	10.1	16.9	22.9	15.2
C_{12}–C_{19} (diesel)	67.8	60.7	54.9	36.8
C_{20+}	21.9	22.3	22.1	47.9
Diesel–naphtha ratio	6.71	3.58	2.40	2.41
Wax conversion (%)	100	95	77	47

Temperature = 300 °C, LHSV = 1

see that for the lower-temperature, lower-conversion levels the heavier products show a similar conversion (Fig. 14). As expected, the intermediate carbon number fraction may become more negative since these components are formed from cracking as well as disappearing due to conversion and transport from the reactor that depends upon VLE effects. As indicated in Fig. 14 (bottom) the intermediate carbon number components do become more negative, indicating they are formed less rapidly by cracking of high carbon number compounds than they exit the reactor as a vapor. Since the feed contains little of the lighter products and because these are formed during cracking reactions, the

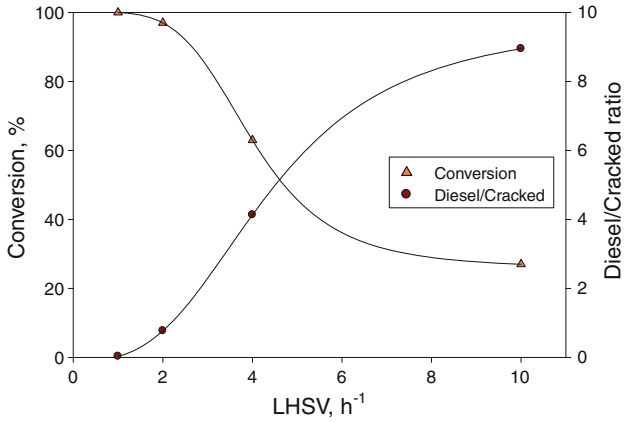

Fig. 13 The dependence of the conversion and the diesel/naphtha ratio in the products on the space velocity

Table 5 The effect of LHSV on hydrocracking reaction over Pt/silica–alumina catalyst

LHSV: Cracking HC (wt%)	1	2	4	10
C_2–C_3	0.76	0.35	0.42	0.13
C_4–C_{11} (naphtha)	96.5	54.7	13.4	6.15
C_{12}–C_{19} (diesel)	2.76	42.2	55.3	55.0
C_{20+}	0	2.75	30.9	38.7
Diesel–naphtha ratio	0.03	0.77	4.13	8.95
Wax conversion (%)	100	97	63	27

Temperature = 300 °C, Pressure = 450 psig

fraction of these products should show a positive increase with increasing conversion, and they do. Thus, the conclusion is that the conversion of the heavier wax components present primarily in the liquid phase react in direct proportion to their concentration in the mixture; that is, a similar, or the same, fraction of each high carbon number component converts during unit time. While the conversion trend for the variation with LHSV is not as clear as anticipated, the trend with increasing conversion is what one would expect (Fig. 15).

4 Summary

As shown in Fig. 3, the conversion of *n*-octacosane is slightly higher than that of *n*-hexadecane but only by a factor of two or so when these reactants are converted alone. Because of the difference in boiling points, we expect *n*-hexadecane to be present in both the liquid and gaseous phases (Fig. 5a) but the *n*-octacosane to be present predominantly in the liquid phase (Fig. 5b). Thus, it appears that under our experimental conditions each reactant saturates the catalytic sites and that the breaking of the C–C bond occurs at roughly the same rate for each

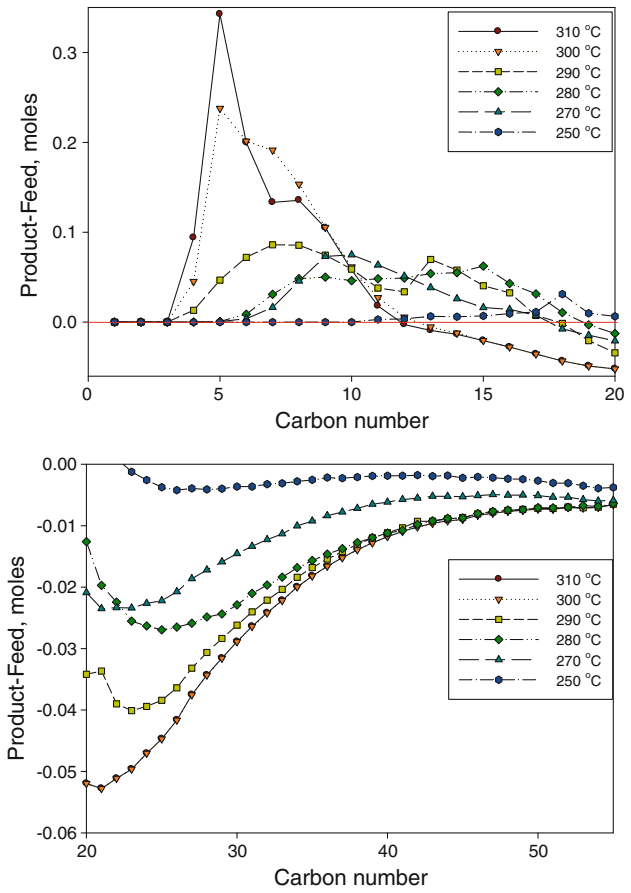

Fig. 14 The product–feed versus carbon number of Co FT wax over Pt/Si–Al catalyst with different temperature at LHSV = 2, pressure = 450 psig, H_2/hydrocarbon = 20 (low carbon number (*top*); high carbon number (*bottom*))

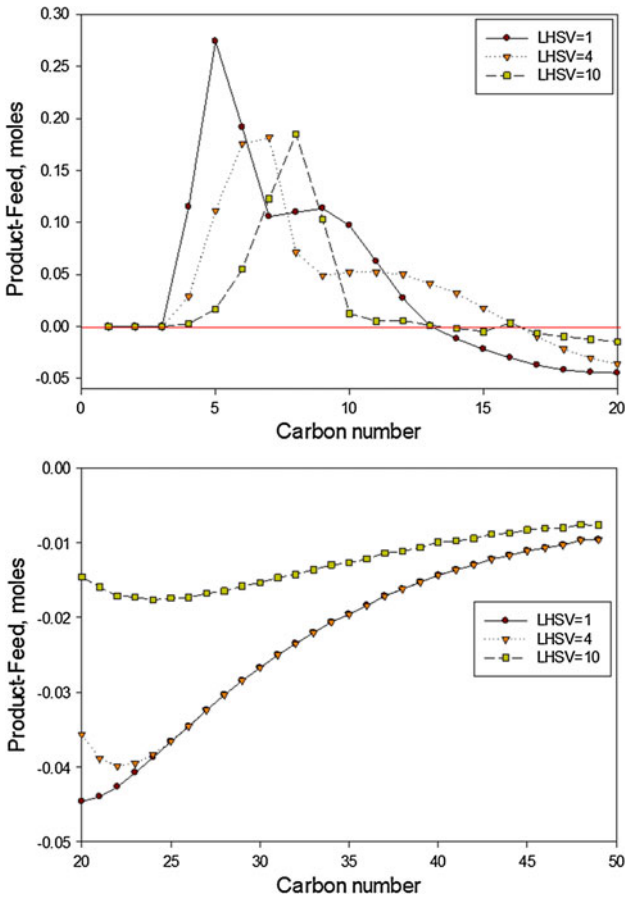

Fig. 15 The product versus carbon number of Co FT wax over Pt/Si–Al catalyst with different LHSV at temperature = 300 °C, pressure = 450 psig, H_2/hydrocarbon = 20 (low carbon number (*top*); high carbon number (*bottom*))

reactant. However, when the mixture is converted, the vapor–liquid equilibrium properties dominate the conversion process. Thus, for an equimolar mixture of these two reactants, the higher carbon number component that is present primarily in the liquid phase dominates the conversion. Thus, in a competitive situation, the solubility of the lower carbon number is insufficient to dominate and the lighter reactant is rapidly transported through the catalyst bed primarily in the vapor phase. This short residence time, relative to the component present predominantly in the liquid phase, limits the conversion of the lower boiling compound and in the present mixture the limit is nearly zero conversion relative to the higher boiling component.

For the ideal catalytic cracking reaction, one expects to form two molecules for each molecule of alkane that is converted by the cracking reaction. Figure 16 shows that the cracking selectivity for *n*-hexadecane is essentially constant over the total conversion range and that about 2.4 mol of products are formed for each *n*-hexadecane that is converted. This means that about 40 % of the carbocation fragments that are formed by the cracking reaction undergo a second isomerization or cracking reaction. Presumably, the cation fragments undergoing the second cracking step are the longer chain ones. For *n*-octacosane, the cracking selectivity is about the same as for *n*-hexadecane for the lowest conversion level but for the higher carbon number reactant the number of moles produced increases with increasing conversion levels of the reactant. Thus, for the *n*-octacosane reactant, a significant fraction of the primary products have a sufficiently high boiling point to remain in the liquid phase long enough to undergo secondary cracking reactions. Furthermore, the relative extents of secondary cracking increase with increasing conversion of the *n*-octacosane.

The FT wax used in this study has a wide range of carbon number compounds. Thus, a small fraction of the components will have a boiling point that is low enough for them to behave similarly to *n*-hexadecane in the competitive conversion situation and to exit the reactor with minimal conversion. On the other hand, most of the sample will have carbon numbers sufficiently high for them to be present predominantly in the liquid phase. Thus, we would

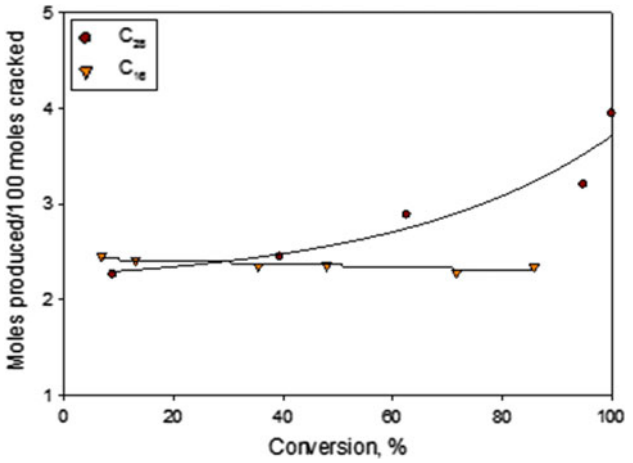

Fig. 16 Produced moles versus 100 mol cracked of C_{16} and C_{28} feeds over Pt/Si–Al catalyst with conversion

expect the conversion fraction for the higher carbon number components to be the same. For the lower conversion levels this appears to be the case. However, the conversion rate of the lower carbon number products ($C_{20–30}$) increases with conversion, showing that these components that have a significant fraction in the vapor phase exit the reactor more rapidly than they undergo secondary cracking reactions.

Acknowledgments This work was supported by the Commonwealth of Kentucky.

References

1. Scherzer J, Gruia AJ (1996) Hydrocracking Science and Technology. Taylor & Francis, Boca Raton
2. de Klerk A, Furimsky E (2010), Catalysis in the refining of Fischer-Tropsch Syncrude, RSC, Cambridge
3. deKlerk A (2011), Fischer-Tropsch Refining, Wiley, Weinheim
4. Coonradt HL, Garwood WE (1964) Ind Eng Chem, Process Des Dev 3:38
5. Weitkamp J (1975) In: Ward JW, Qader SA (eds) Hydrocracking and Hydrotreating, vol 20. American Chemical Society, pp 1–27
6. Weitkamp J, Jacobs PA, Martens JA (1983) Appl Catal 8:123
7. Martens J, Jacobs P, Weitkamp J (1986) Appl Catal 20:239
8. Martens JA, Jacobs P (2001) Stud Surf Sci Catal 137:633
9. Kumar H, Froment GF (2007) Ind Eng Chem Res 46:4075
10. Valery E, Guillaume D, Surla K, Galtier P, Verstraete J, Schweich D (2007) Ind Eng Chem Res 46:4755
11. Leite L, Benazzi E, Marcheal-George N (2001) Catal Today 65:241
12. Sato K, Iwata Y, Yoneda T, Nishijima A, Miki Y, Shimada H (1998) Catal Today 45:367
13. Dupain X, Krul RA, Makkee M, Moulijin JA (2005) Catal Today 106:288
14. Qiu B, Yi X, Lin L, Fang W, Wan H (2008) Catal Today 131:464
15. Blomsma E, Martens JA, Jacobs PA (1997) J Catal 165:241
16. Rezgui Y, Guemini M (2005) Appl Catal A Gen 282:45
17. Fang K, Wei W, Ren J, Sun Y (2004) Catal Lett 93:235
18. Mohanty S, Kunzru D, Saraf DN (1990) Fuel 69:1467
19. Santilli DS, Zones SI (1990) Catal Lett 7:383
20. Calemma V, Peratello S, Perego C (2000) Appl Catal A Gen 190:207
21. Lu Y, He M-Y, Shu X-T, Zong B-N (2003) Energy Fuel 17:1040